

Alma Mater Studiorum Università di Bologna
Archivio istituzionale della ricerca

Peculiar polycyclic aromatic hydrocarbons accumulation patterns in a non-zooxanthellate scleractinian coral

This is the final peer-reviewed author's accepted manuscript (postprint) of the following publication:

Published Version:

Frapiccini, E., Caroselli, E., Franzellitti, S., Prada, F., Marini, M., Goffredo, S. (2022). Peculiar polycyclic aromatic hydrocarbons accumulation patterns in a non-zooxanthellate scleractinian coral. MARINE POLLUTION BULLETIN, 184, 1-8 [10.1016/j.marpolbul.2022.114109].

Availability:

This version is available at: <https://hdl.handle.net/11585/898614> since: 2022-11-28

Published:

DOI: <http://doi.org/10.1016/j.marpolbul.2022.114109>

Terms of use:

Some rights reserved. The terms and conditions for the reuse of this version of the manuscript are specified in the publishing policy. For all terms of use and more information see the publisher's website.

This item was downloaded from IRIS Università di Bologna (<https://cris.unibo.it/>).
When citing, please refer to the published version.

(Article begins on next page)

This is the final peer-reviewed accepted manuscript of:

Frapiccini E., Caroselli E., Franzellitti S., Prada F., Marini M., Goffredo S.: *Peculiar polycyclic aromatic hydrocarbons accumulation patterns in a non-zooxanthellate scleractinian coral*

MARINE POLLUTION BULLETIN 184. ISSN 0025-326X

DOI: 0.1016/j.marpolbul.2022.114109

The final published version is available online at:

<https://dx.doi.org/10.1016/j.marpolbul.2022.114109>

Rights / License:

The terms and conditions for the reuse of this version of the manuscript are specified in the publishing policy. For all terms of use and more information see the publisher's website.

This item was downloaded from IRIS Università di Bologna (<https://cris.unibo.it/>)

When citing, please refer to the published version.

Peculiar polycyclic aromatic hydrocarbons accumulation patterns in a non-zooxanthellate scleractinian coral

Frapiccini Emanuela^{1,4,#}, Caroselli Erik^{2,4,#}, Franzellitti Silvia^{3,4}, Prada Fiorella^{1,4,†}, Marini Mauro^{1,4,*}, Goffredo Stefano^{2,4}

¹ Institute of Biological Resources and Marine Biotechnology (IRBIM), National Research Council (CNR), Largo Fiera della Pesca 2, 60125 Ancona, Italy

² Marine Science Group, Department of Biological, Geological and Environmental Sciences, University of Bologna, via Selmi 3, 40126 Bologna, Italy

³ Animal and Environmental Physiology Laboratory, Department of Biological, Geological and Environmental Sciences, University of Bologna, via S. Alberto 163, 48123 Ravenna, Italy

⁴ Fano Marine Center, The Inter-Institute Center for Research on Marine Biodiversity, Resources and Biotechnologies, Viale Adriatico 1/N 61032 Fano, Italy

[†] Current address: Environmental Biophysics and Molecular Ecology Program, Department of Marine and Coastal Sciences, Rutgers University, New Brunswick, NJ 08901, USA.

[#] Equally contributing authors

^{*} Corresponding author: Mauro Marini, mauro.marini@cnr.it

E-mail Addresses

Emanuela Frapiccini: emanuela.frapiccini@cnr.it; Erik Caroselli: erik.caroselli@unibo.it; Silvia Franzellitti: silvia.franzellitti@unibo.it; Fiorella Prada: fiorella.prada2@unibo.it; Stefano Goffredo: s.goffredo@unibo.it; Mauro Marini: mauro.marini@cnr.it

29 Abstract

30

31 Assessing the sources and accumulation patterns of polycyclic aromatic hydrocarbons (PAHs) in corals is
32 critical, as they threaten coral ecosystem resilience in addition to other anthropogenic pressures. We
33 determined acenaphthene, fluorene, fluoranthene, and pyrene concentration in the skeleton and soft tissue of 7
34 adult and 29 old specimens of the non-zooxanthellate coral *Leptopsammia pruvoti* from the Mediterranean
35 Sea. *Leptopsammia pruvoti* accumulated 2-72 times higher PAH concentrations than the previously
36 investigated zooxanthellate *Balanophyllia europaea* living at the same site at shallower depth, likely in relation
37 to the different trophic strategy. Low molecular weight PAHs were preferentially accumulated compared to
38 high molecular weight PAHs. Detected PAHs were mainly petrogenic, consistently with local pollution
39 sources. Populations of *L. pruvoti* immobilized PAHs in the skeleton 3-4 orders of magnitude more efficiently
40 than *B. europaea*. This highlights the need to investigate other non-zooxanthellate species, which represent the
41 majority of Mediterranean scleractinians, but are widely overlooked with respect to the few zooxanthellate
42 species.

43

44 Keywords (max 6)

45 bioaccumulation; *Leptopsammia pruvoti*; Mediterranean Sea; PAH; QuEChERS; trophic strategy.

46

47

48 1. Introduction

49 Being bioconstructors, corals are extremely ecologically valuable in marine ecosystems, providing habitats for
50 a variety of organisms, and several ecosystem services from a human health and well-being perspective.
51 Nevertheless, they have been subjected to the most extensive and prolonged damage in recent decades
52 (Cornwall et al. 2021; Eddy et al. 2021). Rising sea surface temperatures and ocean acidification are identified
53 as the main environmental drivers of coral and coral reef decline worldwide (Cornwall et al. 2021). Coral
54 disease outbreaks have also relevant implications for reef conservation and restoration (Moriarty et al. 2020).
55 Though mitigating such global stressors remains a priority of conservation efforts, coral-reef managers seek
56 to monitor local stressors to unravel putative synergies with global impacts (Ateweberhan et al. 2013), and to

57 establish effective water quality thresholds to help protect ecosystem function (Nalley et al. 2021). In this
58 regard, the impacts of chemical pollution are gaining attention as they are less understood. Much of the research
59 effort have been addressed to inorganic chemicals, including metals and nutrients, while effects of organic
60 pollutants with bioaccumulative and toxicity features have been poorly explored (Nalley et al. 2021).

61 Polycyclic aromatic hydrocarbons (PAHs; Combi et al., 2020) are the constituents of fuels and oils
62 most harmful to the marine environment (Rocha and Palma, 2019). Natural PAH sources exist (e.g., diagenesis
63 of organic matter, biological processes) but the main source is anthropogenic (Abdel-Shafy and Mansour,
64 2016; Sun et al., 2018), such as incomplete combustion of organic matter and fossil fuels (pyrogenic PAHs)
65 or direct discharge from a variety of sources (petrogenic PAHs) (Abdel-Shafy and Mansour, 2016). Due to
66 their physicochemical characteristics (i.e., octanol-water partition coefficient ranging from 3.2 to 5.4;
67 Frapiccini and Marini 2015), PAHs are easily adsorbed onto suspended particulate matter of the water column
68 and are preferentially partitioned into sediments or biological tissues (Sun et al., 2018), making benthic
69 organisms such as corals particularly subjected to PAH accumulation and toxicity (Caroselli et al., 2020).
70 PAHs interfere with coral gene transcription (Woo et al., 2014), metabolism (Downs et al., 2006; Guzmán
71 Martínez et al., 2007), tissue integrity (Guzmán Martínez et al., 2007; Renegar et al., 2021), larval development
72 and settlement (Negri and Heyward, 2000; Nordborg et al., 2018). Corals can occupy multiple trophic niches
73 thus acquiring pollutants PAHs through multiple pathways, such as direct bioconcentration from seawater or
74 from contact with sediments, and their trophic strategies, which encompass different degree of heterotrophic
75 nutrition (i.e. the capture of suspended particulate matter, herbivory, zooplankton predation) and autotrophy
76 in zooxanthellate corals (i.e. the acquisition of carbon and nutrients from the photosynthetic byproducts of
77 coral endosymbiotic zooxanthellae algae) (Ashok et al., 2022). Different factors (e.g., growth stage, lipid
78 content, trophic strategy) play an important role on PAH accumulation in corals, but further knowledge on
79 these interactions is needed (Li et al., 2021).

80 *Leptopsammia pruvoti* Lacaze-Duthiers, 1897 (Family: Dendrophylliidae) is a gonochoric (Goffredo
81 et al., 2005), solitary, and non-zooxanthellate coral common on rocky bottom in the Mediterranean Sea and
82 the NE Atlantic, reaching abundances of $>10,000$ individuals m^{-2} (Goffredo et al., 2010), at depths from 0 to
83 70 m (Zibrowius, 1980). The demography and skeletal properties of this species are well described (Caroselli
84 et al., 2012). This study focused on acenaphthene, fluorene, fluoranthene and pyrene to allow a direct

comparison with previous analyses on the zooxanthellate *Balanophyllia europaea*, which preferentially accumulated PAHs in the zooxanthellae, followed by the soft tissue, and the skeleton (Caroselli et al., 2020). As this accumulation pattern seems widespread (Ko et al., 2014; Ranjbar Jafarabadi et al., 2018), this study aimed to assess the influence of heterotrophy on PAH levels and accumulation pattern in *L. pruvoti* and confirm that skeletal storage of PAHs may be related to the coral age population structure, as previously reported for *B. europaea* (Caroselli et al. 2020), thus assessing its impact on PAH contamination in reef ecosystems. Overall, we aimed to assess coral PAH contamination in the Mediterranean Sea, a hotspot for both PAH pollution and climate change (Diffenbaugh et al., 2007; Castro-Jiménez et al., 2012), where more than 90% of existing scleractinian coral species are non-zooxanthellate such as *L. pruvoti* (Zibrowius, 1980).

2. Materials and Methods

2.1 Sample collection and processing

On June 12th, 2020, scuba divers haphazardly collected thirty-six *L. pruvoti* individual polyps at 16 m depth in Calafuria (Fig. 1), receiving sediments and pollutants from one of the most polluted port areas in Italy (Bertolotto et al., 2003; Iannelli et al., 2012). Upon collection, samples were transferred to the laboratory and stored at -20°C.

The maximum oral disc length of the (*L*) of each coral was measured with Vernier calipers (Caroselli et al. 2012). The von Bertalanffy length-age relationship of this *L. pruvoti* population was applied to estimate the age of each coral (Goffredo et al., 2010), and samples were categorized either in the age class Adult ($2 < \text{age (years)} \leq 4$; $N = 7$) or Old ($4 < \text{age (years)} \leq 7$; $N = 29$). Coral soft tissue was separated with an airbrush methods and coral skeletons were bleached by immersion in a 10% sodium hypochlorite (commercial bleach) solution for 3 days, dried in an oven at 50°C for three days, and then powdered with an agate mortar (Caroselli et al. 2020). Lyophilized soft tissue and powdered skeletons were weighed with a precision balance (± 0.0001 g, Scaltec) and the intra-skeletal organic matrix (OM) dry mass was assumed as 2.5% of skeletal mass (Reggi et al., 2014). Skeletal PAH concentration of samples was normalized over OM dry mass.

2.2 PAH quantification

112 Acenaphthene, fluorene, fluoranthene and pyrene were extracted and purified from skeleton and soft tissue
113 samples using Quick Easy Cheap Effective Rugged and Safe (QuEChERS) method (Table A.1; Caroselli et
114 al. 2020). All laboratory blanks were below the limit of quantification (LOQ). The population age structure,
115 coral length, and skeletal mass at each age class of this *L. pruvoti* population (Goffredo et al., 2010) were used
116 to quantify the amount of each PAH stored in 1 m² (for the calculation see Caroselli et al. 2020).

117

118 2.3 Statistical analyses

119 Concentration data were heteroskedastic and were thus compared with a permutation multivariate analysis of
120 variance (PERMANOVA; Anderson, 2005) using Euclidean distances with software Primer 6 (Primer-e Ltd).
121 The crossed design used three fixed factors (“PAH” with four levels: acenaphthene, fluorene, fluoranthene,
122 pyrene; “Compartment” with 2 levels: Skeleton, Tissue; and “Age class” with 2 levels: Adult, Old), 999
123 permutations, and the Monte Carlo p-value correction due to the small sample size. A further PERMANOVA
124 analysis with analogous settings and the factors Compartment and Age class was performed separately for
125 each PAH.

126

127 3. Results

128 Acenaphthene, fluorene, fluoranthene, and pyrene concentration in the skeleton and tissue of 7 adult and 29
129 old individuals of *L. pruvoti* was quantified (Table 1; Table A.2). In both biological compartments, the
130 dominant PAH was acenaphthene, followed by fluorene, fluoranthene and pyrene (Fig. 2). Fluoranthene and
131 pyrene generally had lower concentration than fluorene and acenaphthene (Fig. 2; Table 2; Table A.3). The
132 concentration of pyrene was lower in the skeleton than in the tissue, while an opposite pattern was observed
133 for acenaphthene (Fig. 2; Table A.4). Fluorene and fluoranthene concentrations were homogeneous in the two
134 compartments (Fig. 2; Table A.4). These findings were also confirmed by the analysis on individual PAHs
135 (Table 3). Age was always not significant (Table 2, Table 3).

136 To discriminate petroleum and combustion sources of the investigated PAHs, the
137 *anthracene/(anthracene+phenanthrene)* diagnostic ratios were plotted against the
138 *fluoranthene/(fluoranthene+pyrene)* ones (Fig. 3; Maletic et al., 2019). PAHs in 91.2% of skeletal samples
139 showed *anthracene/(anthracene+phenanthrene)* values below 0.1, an indication of petroleum origin, while

140 2.9% had a pyrogenic origin and 5.9% a mixed origin, with a strong predominance of petrogenic PAHs in the
141 skeleton (χ^2 test, $p < 0.001$; Fig. 3). In the tissue, the petrogenic origin was still dominant among samples
142 (50.0%), with 34.4% having a pyrogenic component and 15.6% a mixed origin, but in this case the difference
143 between petrogenic and pyrogenic origin was not statistically significant (χ^2 test, $p > 0.05$; Fig. 3).

144 Coral skeletons in one square meter of this *L. pruvoti* population were estimated to store 355.3 μg of
145 acenaphthene, 52.0 μg of fluorene, 9.2 μg of fluoranthene, and 7.8 μg of pyrene (Fig. 4; Table A.5).

146

147 4. Discussion

148 This first investigation of PAHs in a non-zooxanthellate coral species observed that *Leptopsammia pruvoti*
149 specimens accumulated PAHs up to about 10 $\mu\text{g g}^{-1}$ dry weight (d.w.) in their skeletons. The mainly petrogenic
150 origin of detected PAHs confirms the previous study on *B. europaea* in the same area, suggesting the presence
151 of petroleum contamination at the sampling site (Caroselli et al., 2020). A preferential accumulation of the low
152 molecular weight PAHs fluorene and acenaphthene was observed, as in the zooxanthellate coral *B. europaea*
153 collected at the same site at shallower depths (i.e., 6 m; Caroselli et al., 2020) and in tropical corals (Ko et al.,
154 2014; Ranjbar Jafarabadi et al., 2018; Han et al., 2020), likely due to their higher solubility (Sverdrup et al.,
155 2002).

156 PAH concentration in *L. pruvoti* was 2-72 times higher than in the analogous compartments of *B.*
157 *europaea* (Table 1; Caroselli et al. 2020) and ranged similarly to Red Sea corals (0.007-0.308 vs. 0.03–0.3 μg
158 g^{-1} over skeletal dry weight, respectively; El-Sikaily et al., 2003). Since *B. europaea* and *L. pruvoti* were
159 collected within a few tens of meters, and within 10 m of the water column (6 m vs 16 m), their different
160 concentration is unlikely ascribable to a different environmental burden of PAHs. A possible explanation to
161 the observed differences between *L. pruvoti* and *B. europaea* could depend on their different energy intake
162 strategies and therefore different trophic position and food-chain. Zooxanthellate corals like *B. europaea* can
163 obtain most of the animal host's metabolic energy needs through translocation of photosynthate by the
164 symbiotic algae (Muscatine 1990), while non-zooxanthellate corals such as *L. pruvoti* feed exclusively on
165 external particulate food sources such as phyto- and zooplankton or detrital organic matter (Ferrier-Pagés and
166 Leal 2019). PAHs adsorbed by particulate matter in the water column (Li et al. 2020) are uptaken by phyto-
167 and zooplankton both directly from seawater and by feeding (Hsieh et al., 2019), with potential further transfer

168 to low-level trophic webs (Alekseenko et al., 2018). The accumulation of the PAH phenanthrene in the tropical
169 coral *Acropora millepora* under three treatments representing PAH exposure levels of increasing food-chain
170 length (i.e., dissolved in seawater, exposed microalgae representing herbivory, and exposed copepods
171 representing predation) showed increased bioaccumulation in the treatment with PAH exposed copepods (i.e.,
172 with increased food-chain length) (Ashok et al. 2022). Thus, the increased food-chain length in *L. pruvoti*
173 (exclusively heterotrophic) compared to *B. europaea* (mixotrophic) could partially explain the higher PAH
174 accumulation in the former compared to the latter. The routes of initial PAH uptake of both species are likely
175 to be the same (i.e., either feeding or through direct adsorption from the dissolved fraction). However, the
176 balance of uptake routes is likely to differ as *L. pruvoti* relies solely on heterotrophy.

177 The different trophic strategies could also explain the different PAH accumulation pattern among
178 tissue and skeleton in *L. pruvoti* and *B. europaea*. PAH accumulation pattern of all previously investigated
179 corals from different locations is zooxanthellae > coral tissue > coral skeleton (Ko et al., 2014; Ranjbar
180 Jafarabadi et al., 2018; Caroselli et al. 2020). Acenaphthene was the only PAH exhibiting this pattern in *L.*
181 *pruvoti*. Pyrene was more concentrated in the skeleton than in the tissue, and both fluorene and fluoranthene
182 were equally abundant in the two coral compartments. A recent model for zooxanthellate corals proposes that
183 PAHs are transferred from zooxanthellae to the coral tissue through lipid storage, possibly following the
184 translocation pathways of photosynthetic products from the symbiont to the host (Muscatine et al., 1981, 1984),
185 and then to the final storage in skeleton and associated OM (Caroselli et al., 2020). Heterotrophic corals such
186 as *L. pruvoti* or corals living at different depths (e.g., shallow vs deep) likely have different food webs and
187 their PAH accumulation patterns may consequently differ, according to the zooplankton species involved.
188 Different metabolic pathways, particularly those related to lipid biosynthesis and catabolism, should also be
189 considered. Fatty acid compositions of skeletal OM is different between zooxanthellate and non-zooxanthellate
190 corals, likely linked to the different energy intake strategies, and some are exclusively produced by either the
191 symbiont or the host (Samorì et al., 2017). Thus, exchange of macromolecules between symbionts and the host
192 in zooxanthellate species may determine different PAH accumulation patterns between biological
193 compartments than in non-zooxanthellate species. Further accumulation pattern variability may derive from
194 PAH interaction with mucus (Han et al., 2020), recirculation among biological compartments, and

195 detoxification/biotransformation mechanisms, for which data on corals are still very scarce (Downs et al.
196 2012).

197 The long-term (13 years = maximum estimated longevity; Goffredo et al., 2010) PAH sequestration
198 capacity of this populations of *L. pruvoti* reached a maximum in 4 years old individuals. Considering that
199 PAHs enclosed within the calcium carbonate skeletal crystals are stored until death and further skeletal
200 dissolution, it is important to quantify the extent of these processes under ocean acidification scenarios (IPCC,
201 2019). Since growth and population dynamics are characterized in *L. pruvoti* populations throughout the
202 latitudinal extension of Italian coasts (>1000 km; Caroselli et al. 2012), the ongoing PAH assessment across
203 this gradient may accurately evaluate coral potential to mitigate PAH pollution. It is noteworthy that the 1 m²-
204 normalized amount of PAH stored by *L. pruvoti* populations is 3-4 orders of magnitude higher than in *B.*
205 *europaea* (Table A.5; Caroselli et al. 2020). The possible role of trophic strategies in influencing corals PAH
206 accumulation demands further research to verify if this pattern is ubiquitous or peculiar for *L. pruvoti* and *B.*
207 *europaea* (this study; Caroselli et al. 2020).

208

209 **5. Conclusions**

210 The non-zooxanthellate coral *L. pruvoti* accumulated acenaphthene, fluorene, fluoranthene and
211 pyrene at higher concentrations than the zooxanthellate *B. europaea* (i.e., mixotrophic) living in the
212 same site at shallower depth, likely in relation to the different trophic strategy (i.e., heterotrophy).
213 Populations of the non-zooxanthellate *L. pruvoti* analyzed in this study immobilized PAHs in the
214 skeleton much more efficiently than their zooxanthellate and sympatric counterpart *B. europaea*. This
215 study highlights the need for further research efforts on: i) the overlooked non-zooxanthellate corals,
216 as they represent the vast majority of Mediterranean scleractinian coral species (Zibrowius 1980); ii)
217 the different pathways by which corals accumulate PAHs; iii) the impact of different exposure modes
218 on coral physiology; iv) PAH environmental concentrations in seawater around Mediterranean
219 coralligenous assemblages, which are among the most threatened habitats in the Mediterranean Sea
220 (Ingrosso et al. 2018); and v) analytically-verified biological endpoints suitable for risk assessments,
221 urgently needed to identify local management strategies that prioritize the most important chemical

222 contaminants of concern for marine ecosystems health. These knowledge gaps should also be
223 addressed within the framework of future climate change scenarios and how the accumulation of
224 these pollutants in marine organisms will interact with varying environmental conditions such as
225 ocean warming and acidification.

226

227 **Acknowledgements**

228 The authors declare no competing financial interests. The Scientific Diving School supplied technical and
229 logistical support. The experiments comply with current Italian law.

230

231 **Competing interest statement**

232 The authors declare no competing interest.

233

234

235 **Author contributions**

236 **Frapiccini Emanuela:** Methodology, Investigation, Writing - Review and Editing, Visualization. **Caroselli**
237 **Erik:** Methodology, Formal analysis, Resources, Writing - Review and Editing, Visualization. **Franzellitti**
238 **Silvia:** Methodology, Resources, Writing - Review and Editing. **Prada Fiorella:** Writing - Review and
239 Editing. **Marini Mauro:** Conceptualization, Resources, Writing - Review and Editing, Supervision. **Goffredo**
240 **Stefano:** Conceptualization, Resources, Writing - Review and Editing, Supervision.

241

242

243 **References**

- 244 Abdel-Shafy HI, Mansour MS (2016) A review on polycyclic aromatic hydrocarbons: source, environmental
 245 impact, effect on human health and remediation. Egypt J Pet 25:107-123. doi: 10.1016/j.ejpe.2015.03.011
- 246 Airi V, Prantoni S, Calegari M, Lisini Baldi V, Gizzi F, Marchini C, Levy O, Falini G, Dubinsky Z, Goffredo
 247 S (2017) Reproductive output of a non-zooxanthellate temperate coral is unaffected by temperature along
 248 an extended latitudinal gradient. PLoS ONE, 12: e0171051. doi: 10.1371/journal.pone.0171051
- 249 Alekseenko E, Thouvenin B, Tronczyński J, Carlotti F, Garreau P, Tixier C, Baklouti M (2018) Modeling of
 250 PCB trophic transfer in the Gulf of Lions; 3D coupled model application. Mar Pollut Bull 128:140-155.
 251 doi: 10.1016/j.marpolbul.2018.01.008
- 252 Anderson MJ (2005) PERMANOVA: A FORTRAN computer program for permutational multivariate
 253 analysis of variance. Department of Statistics, Univ. of Auckland.
- 254 Ashok A, Høj L, Brinkman DL, Negri AP, Agusti S (2022) Food-chain length determines the level of
 255 phenanthrene bioaccumulation in corals. Environ Pollut 297:118789. doi: 10.1016/j.envpol.2022.118789
- 256 Ateweberhan M, Feary DA, Keshavmurthy S, Chen A, Schleyer MH, Sheppard CRC (2013) Climate change
 257 impacts on coral reefs: synergies with local effects, possibilities for acclimation, and management
 258 implications. Mar Pollut Bull 74:526-539. doi: 10.1016/j.marpolbul.2013.06.011
- 259 Bertolotto RM, Ghioni F, Frignani M, Alvarado-Aguilar D, Bellucci LG, Cuneo C, Picca MR, Gollo E (2003)
 260 Polycyclic aromatic hydrocarbons in surficial coastal sediments of the Ligurian Sea. Mar Pollut Bull
 261 46:907–913. doi: 10.1016/S0025-326X(03)00114-0
- 262 Caroselli E, Zaccanti F, Mattioli G, Falini G, Levy O, Dubinsky Z, Goffredo S (2012) Growth and demography
 263 of the solitary scleractinian coral *Leptopsammia pruvoti* along a sea surface temperature gradient in the
 264 Mediterranean Sea. PLoS ONE 7:e37848. doi: 10.1371/journal.pone.0037848
- 265 Caroselli E, Frapiccini E, Franzellitti S, Palazzo Q, Prada F, Betti M, Goffredo S, Marini M (2020)
 266 Accumulation of PAHs in the tissues and algal symbionts of a common Mediterranean coral: skeletal
 267 storage relates to population age structure. Sci Total Environ 743:140781. doi:
 268 https://doi.org/10.1016/j.scitotenv.2020.140781

269 Castro-Jiménez J, Berrojalbiz N, Wollgast J, Dachs J (2012) Polycyclic aromatic hydrocarbons (PAHs) in the
 270 Mediterranean Sea: atmospheric occurrence, deposition and decoupling with settling fluxes in the water
 271 column. *Environ Pollut* 166:40-47. doi: 10.1016/j.envpol.2012.03.003.

272 Combi T, Pintado-Herrera MG, Lara-Martín PA, Lopes-Rocha M, Miserocchi S, Langone L, Guerra R (2020)
 273 Historical sedimentary deposition and flux of PAHs, PCBs and DDTs in sediment cores from the western
 274 Adriatic Sea. *Chemosphere* 241:125029. doi: 10.1016/j.chemosphere.2019.125029

275 Cornwall CE, Comeau S, Kornder NA, Perry CT, van Hooidonk R, DeCarlo TM, Pratchett MS, Anderson KD,
 276 Browne N, Carpenter R, Diaz-Pulido G, D’Olivo JP, Doo SS, Figueiredo J, Fortunato SAV, Kennedy E,
 277 Lantz CA, McCulloch MT, González-Rivero M, Schoepf V, Smithers SG, Lowe RJ (2021) Global declines
 278 in coral reef calcium carbonate production under ocean acidification and warming. *Proc Natl Acad Sci*
 279 USA, 118:e2015265118. doi: 10.1073/pnas.2015265118

280 Diffenbaugh NS, Pal JS, Giorgi F, Gao X (2007) Heat stress intensification in the Mediterranean climate
 281 change hotspot. *Geophys Res Lett* 34:L11706. doi: 10.1029/2007GL030000.

282 Downs CA, Richmond RH, Mendiola WJ, Rougee L, Ostrander GK (2006) Cellular physiological effects of
 283 the MV Kyowa Violet fuel-oil spill on the hard coral, *Porites lobata*. *Environ Toxicol Chem* 25:3171–
 284 3180. doi: 10.1897/05-509R1.1

285 Downs CA, Ostrander GK, Rougee L, Rongo T, Knutson S, Williams DE, Mendiola W, Holbrook
 286 J, Richmond RH (2012) The use of cellular diagnostics for identifying sub-lethal stress in reef corals.
 287 *Ecotoxicology* 21:768-82. doi: 10.1007/s10646-011-0837-4

288 Eddy TD, Lam VWY, Reygondeau G, Cisneros-Montemayor AM, Greer K, Palomares MLD, Bruno JF, Ota
 289 Y, Cheung WWL (2021) Global decline in capacity of coral reefs to provide ecosystem services. *One Earth*
 290 4:1278–1285. doi:10.1016/j.oneear.2021.08.016

291 El-Sikaily A, Khaled A, El Nemr A, Said TO, Abd-Alla AMA (2003) Polycyclic aromatic hydrocarbons and
 292 aliphatics in the coral reef skeleton of the Egyptian Red Sea Coast. *Bull Environ Con Tox* 71:1252-1259.
 293 doi: 10.1007/s00128-003-8736-x

294 Ferrier-Pagès C, Leal MC (2019) Stable isotopes as tracers of trophic interactions in marine mutualistic
 295 symbioses. *Ecol Evol* 9:723-740. doi: 10.1002/ece3.4712

296 Frapiccini E, Marini M (2015) Polycyclic aromatic hydrocarbon degradation and sorption parameters in coastal
 297 and open-sea sediment. *Water Air Soil Pollut* 226:246. doi: 10.1007/s11270-015-2510-7

298 Goffredo S, Radetić J, Airi V, Zaccanti F (2005) Sexual reproduction of the solitary sunset cup coral
 299 *Leptopsammia pruvoti* (Scleractinia, Dendrophylliidae) in the Mediterranean. 1. Morphological aspects of
 300 gametogenesis and ontogenesis. *Mar Biol* 147:485-495. doi: 10.1007/s00227-005-1567-z

301 Goffredo S, Caroselli E, Mattioli G, Zaccanti F (2010) Growth and population dynamic model for the non-
 302 zooxanthellate temperate solitary coral *Leptopsammia pruvoti* (Scleractinia, Dendrophylliidae). *Mar Biol*
 303 157:2603-2612. doi: 10.1007/s00227-010-1522-5

304 Guzmán Martínez MDC, Ramírez Romero P, Banaszak AT (2007) Photoinduced toxicity of the polycyclic
 305 aromatic hydrocarbon, fluoranthene, on the coral, *Porites divaricata*. *J Environ Sci Health Part A* 42:1495-
 306 1502. doi: 10.1080/10934520701480946

307 Han M, Zhang R, Yu K, Li A, Wang Y, Huang X (2020) Polycyclic aromatic hydrocarbons (PAHs) in corals
 308 of the South China Sea: Occurrence, distribution, bioaccumulation, and considerable role of coral mucus.
 309 *J Hazard Mater* 384:121299. doi: 10.1016/j.jhazmat.2019.121299

310 Hsieh H-Y, Huang K-C, Cheng J-O, Lo W-T, Meng P-J, Ko F-C (2019) Environmental effects on the
 311 bioaccumulation of PAHs in marine zooplankton in Gaoping coastal waters, Taiwan: Concentration,
 312 distribution, profile, and sources. *Mar Pollut Bull* 144:68-78. doi: 10.1016/j.marpolbul.2019.04.048

313 Iannelli R, Bianchi V, Macci C, Peruzzi E, Chiellini C, Petroni G, Masciandaro G (2012) Assessment of
 314 pollution impact on biological activity and structure of seabed bacterial communities in the Port of Livorno
 315 (Italy). *Sci Total Environ* 426:56–64. doi: 10.1016/j.scitotenv.2012.03.033

316 Ingrosso G, Abbiati M, Badalamenti F, Bavestrello G, Belmonte G, Cannas R, Benedetti-Cecchi L, Bertolino
 317 M, Bevilacqua S, Nike Bianchi C, Bo M, Boscari E, Cardone F, Cattaneo-Vietti R, Cau A, Cerrano C,
 318 Chemello R, Chimienti G, Congiu L, Corriero G, Costantini F, De Leo F, Donnarumma L, Falace A,
 319 Frascetti S, Giangrande A, Gravina MF, Guarnieri G, Mastrototaro F, Milazzo M, Morri C, Musco L,
 320 Pezzolesi L, Piraino S, Prada F, Ponti M, Rindi F, Russo GF, Sandulli R, Villamor A, Zane L, Boero F
 321 (2018) Mediterranean bioconstructions along the Italian coast. *Adv Mar Biol* 79:61-136. doi:
 322 10.1016/bs.amb.2018.05.001

IPCC (2019) IPCC Special Report on the Ocean and Cryosphere in a Changing Climate. Pörtner H-O, Roberts DC, Masson-Delmotte V, Zhai P, Tignor M, Poloczanska E, Mintenbeck K, Alegría A, Nicolai M, Okem A, Petzold J, Rama B, Weyer NM (eds.). In press.

Ko F-C, Chang C-W, Cheng J-O (2014) Comparative study of polycyclic aromatic hydrocarbons in coral tissues and the ambient sediments from Kenting National Park, Taiwan. *Environ Pollut* 185:35-43. doi: 10.1016/j.envpol.2013.10.025

Li H, Duan D, Beckingham B, Yang Y, Ran Y, Grathwohl P (2020) Impact of trophic levels on partitioning and bioaccumulation of polycyclic aromatic hydrocarbons in particulate organic matter and plankton. *Mar Pollut Bull* 160:111527. doi: 10.1016/j.marpolbul.2020.111527

Li Y, Zou X, Zou S, Li P, Yang Y, Wang J (2021) Pollution status and trophic transfer of polycyclic aromatic hydrocarbons in coral reef ecosystems of the South China Sea. *ICES J Mar Sci* 78:2053–2064. doi: 10.1093/icesjms/fsab081

Maletić SP, Beljin JM, Rončević SD, Grgić MG, Dalmacija BD (2019) State of the art and future challenges for polycyclic aromatic hydrocarbons in sediments: sources, fate, bioavailability and remediation techniques. *J Hazard Mater* 365:467-482. doi: 10.1016/j.jhazmat.2018.11.020

Moriarty T, Leggat W, Huggett MJ, Ainsworth TD (2020) Coral disease causes, consequences, and risk within coral restoration. *Trends Microbiol* 28:793-807. doi: 10.1016/j.tim.2020.06.002

Muscattine L, McCloskey LR, Marian RE (1981) Estimating the daily contribution of carbon from zooxanthellae to coral animal respiration. *Limnol Oceanogr* 26:601-611. doi: 10.4319/lo.1981.26.4.0601

Muscattine L, Falkowski PG, Porter JW, Dubinsky Z (1984) Fate of photosynthetic fixed carbon in light- and shade-adapted colonies of the symbiotic coral *Stylophora pistillata*. *Proc R Soc Lond B* 222:181–202. doi: 10.1098/rspb.1984.0058

Muscattine L (1990) The role of symbiotic algae in carbon and energy flux in reef corals. In: Dubinsky Z (Ed.), *Ecosystems of the World. Coral Reefs*, pp. 75–87.

Nalley EM, Tuttle LJ, Barkman AL, Conklin EE, Wulstein DM, Richmond RH, Donahue MJ (2021) Water quality thresholds for coastal contaminant impacts on corals: A systematic review and meta-analysis. *Sci Total Environ* 794:148632. doi: 10.1016/j.scitotenv.2021.148632

350 Negri AP, Heyward AJ (2000) Inhibition of fertilization and larval metamorphosis of the coral *Acropora*
351 *millepora* (Ehrenberg, 1834) by petroleum products. Mar Pollut Bull 41:420-427. doi: 10.1016/S0025-
352 326X(00)00139-9

353 Nordborg FM, Flores F, Brinkman DL, Agustí S, Negri AP (2018) Phototoxic effects of two common marine
354 fuels on the settlement success of the coral *Acropora tenuis*. Sci Rep 8:8635. doi: 10.1038/s41598-018-
355 26972-7

356 Ranjbar Jafarabadi A, Riyahi Bakhtiari A, Aliabadian M, Laetitia H, Shadmehri Toosi A, Yap CK (2018) First
357 report of bioaccumulation and bioconcentration of aliphatic hydrocarbons (AHs) and persistent organic
358 pollutants (PAHs, PCBs and PCNs) and their effects on alcyonacea and scleractinian corals and their
359 endosymbiotic algae from the Persian Gulf, Iran: Inter and intra-species differences. Sci Total Environ
360 627:141-157. doi: 10.1016/j.scitotenv.2018.01.185

361 Reggi M, Fermani S, Landi V, Sparla F, Caroselli E, Gizzi F, Dubinsky Z, Levi O, Cuif JP, Dauphin Y,
362 Goffredo S, Falini G (2014) Biomineralization in Mediterranean corals: The role of the intra-skeletal
363 organic matrix. Cryst Growth Des 14:4310-4320. doi: 10.1021/cg5003572

364 Renegar DA, Turner NR (2021) Species sensitivity assessment of five Atlantic scleractinian coral species to
365 1-methylnaphthalene. Sci Rep 11:529. doi: 10.1038/s41598-020-80055-0

366 Rocha AC, Palma C (2019) Source identification of polycyclic aromatic hydrocarbons in soil sediments:
367 Application of different methods. Sci Total Environ 652:1077-1089. doi: 10.1016/j.scitotenv.2018.10.014

368 Samorì C, Caroselli E, Prada F, Reggi M, Fermani S, Dubinsky Z, Goffredo S, Falini G (2017) Ecological
369 relevance of skeletal fatty acid concentration and composition in Mediterranean scleractinian corals. Sci
370 Rep 7:1929. doi:10.1038/s41598-017-02034-2

371 Sun RX, Sun Y, Li QX, Zheng X, Luo X, Mai B (2018) Polycyclic aromatic hydrocarbons in sediments and
372 marine organisms: Implications of anthropogenic effects on the coastal environment. Sci Total Environ
373 640-641:264-272. doi: 10.1016/j.scitotenv.2018.05.320

374 Sverdrup LE, Nielsen T, Krogh PH (2002) Soil ecotoxicity of Polycyclic Aromatic Hydrocarbons in relation
375 to soil sorption, lipophilicity and water solubility. Environ Sci Technol 36:2429-2435. doi:
376 10.1021/es010180s

377 Woo S, Lee A, Denis V, Chen CA, Yum S (2014) Transcript response of soft coral (*Scleronephthya*
378 *gracillimum*) on exposure to polycyclic aromatic hydrocarbons. Environ Sci Pollut Res 21:901–910. doi:
379 10.1007/s11356-013-1958-5
380 Zibrowius H (1980) Les scleractiniaires de la Mediterraee et de l’Atlantique nord-oriental. Mem Inst Oceanogr
381 Monaco 11:1–284
382

383 Tables

384 **Table 1** Concentration ($\mu\text{g g}^{-1}$ dry weight, d.w.) of the four PAHs in the biological compartments and in the
 385 two age classes of *L. pruvoti* specimens. Analogous data for *B. europaea* are added for comparison (Caroselli
 386 et al., 2020). Values are indicated as means with 95% Confidence Intervals in parentheses. N: Number of
 387 samples.

		N	acenaphthene ($\mu\text{g g}^{-1}$ d.w.)	fluorene ($\mu\text{g g}^{-1}$ d.w.)	fluoranthene ($\mu\text{g g}^{-1}$ d.w.)	pyrene ($\mu\text{g g}^{-1}$ d.w.)
<i>Leptopsammia pruvoti</i>						
	Adult	7	12 (8-17)	1.7 (1.0-2.5)	0.25 (0.11-0.39)	0.25 (0.10-0.40)
Skeleton	Old	29	12 (10-15)	1.8 (1.5-2.1)	0.33 (0.25-0.41)	0.27 (0.16-0.38)
	Total	36	12 (10-15)	1.8 (1.5-2.1)	0.32 (0.25-0.39)	0.27 (0.18-0.36)
	Adult	7	3.3 (0.0-7.6)	3.1 (0.0-6.5)	0.73 (0.01-1.46)	0.86 (0.0-1.79)
Tissue	Old	29	4.1 (1.5-6.7)	3.0 (0.8-5.2)	0.33 (0.17-0.50)	0.35 (0.18-0.53)
	Total	36	4.0 (1.7-6.2)	3.0 (1.2-4.9)	0.41 (0.22-0.60)	0.45 (0.22-0.68)
<i>Balanophyllia europaea</i>						
	Adult	6	0.21 (0.08-0.35)	0.24 (0.12-0.36)	0.01 (0.01-0.01)	0.04 (0.03-0.05)
Skeleton	Old	7	0.13 (0.10-0.16)	0.20 (0.11-0.29)	0.01 (0.01-0.01)	0.03 (0.02-0.04)
	Total	13	0.17 (0.15-0.23)	0.22 (0.15-0.29)	0.01 (0.01-0.01)	0.04 (0.03-0.04)
	Adult	6	0.17 (0.12-0.22)	0.51 (0.34-0.69)	0.01 (0.00-0.02)	0.07 (0.03-0.12)
Tissue	Old	7	0.55 (0.05-1.04)	1.2 (0.4-2.1)	0.08 (0.05-0.10)	0.28 (0.15-0.42)
	Total	13	0.37 (0.09-0.65)	0.89 (0.41-1.37)	0.05 (0.03-0.07)	0.19 (0.09-0.28)
	Adult	6	1.1 (0.4-1.7)	2.1 (1.0-3.2)	0.09 (0.05-0.12)	0.57 (0.00-1.15)
Zooxanthellae	Old	7	0.77 (0.20-1.34)	2.1 (0.9-3.2)	0.29 (0.13-0.45)	1.0 (0.6-1.5)
	Total	13	0.91 (0.48-1.33)	2.1 (1.3-2.9)	0.20 (0.10-0.30)	0.82 (0.46-1.18)

388

389

390 **Table 2** Results of the comparative PERMANOVA analysis for PAH concentration.

Factor	df	Pseudo-F	P
PAH	3	32.735	0.001
Compartment	1	6.9438	0.011
Age class	1	0.0013	0.975
PAH x Compartment	3	13.392	0.001
PAH x Age class	3	0.0707	0.973
Age class x Compartment	1	0.0100	0.938
PAH x Age class x Compartment	3	0.0490	0.977

391 df: degrees of freedom; Pseudo-F: F value by permutation (Anderson et al., 2005); P: significance of pseudo-
392 F with Monte Carlo correction.

393

394

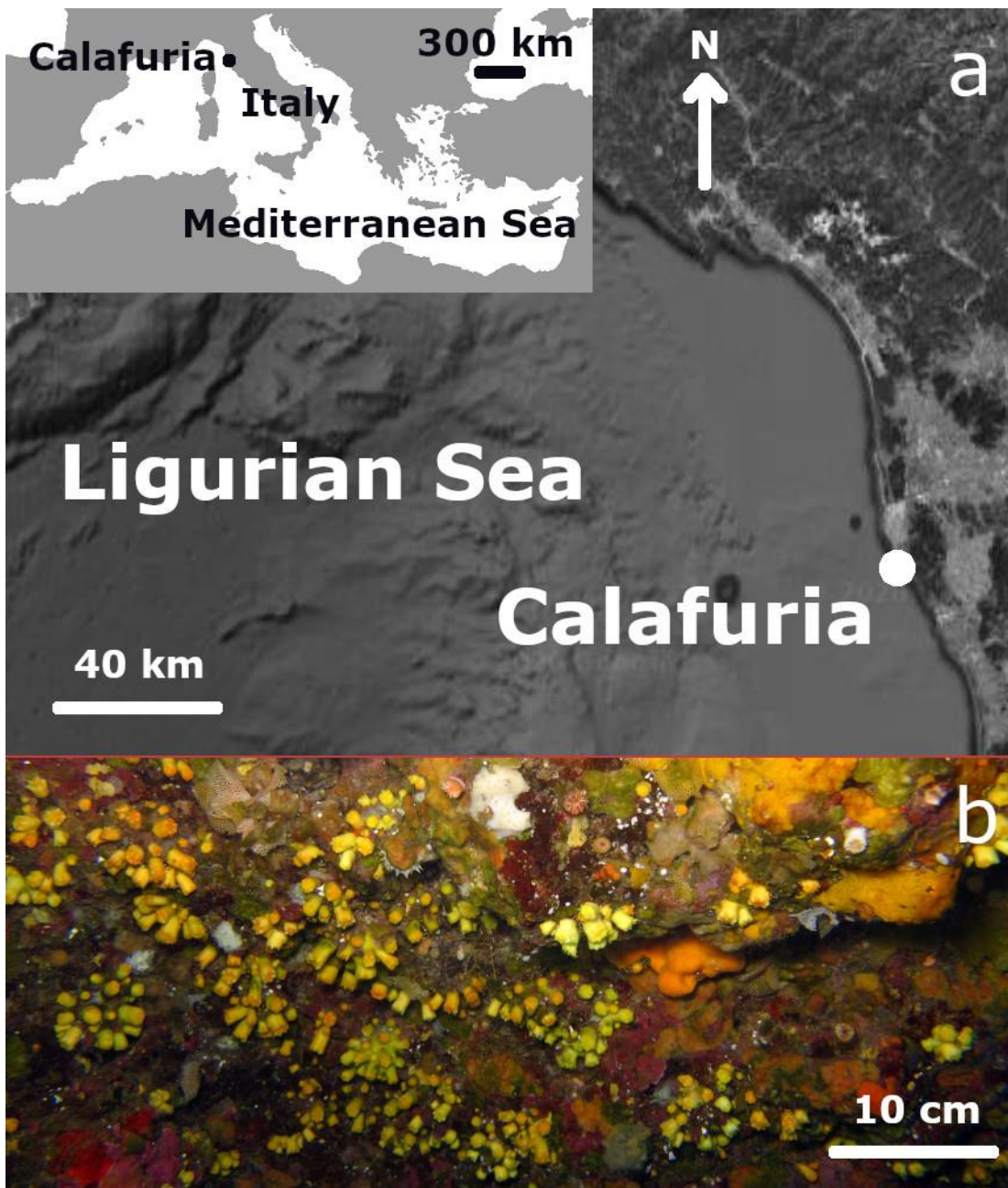
395

396 **Table 3** Results of the PERMANOVA analysis for the concentration of each of the four PAHs.

Factor	acenaphthene			fluorene		fluoranthene		pyrene	
	df	Pseudo-F	P	Pseudo-F	P	Pseudo-F	P	Pseudo-F	P
Compartment	1	15.444	0.001	1.069	0.308	3.431	0.065	4.914	0.033
Age class	1	0.053	0.818	2.73E ⁻⁰⁶	0.998	1.465	0.247	2.427	0.134
Compartment x Age class	1	0.024	0.877	0.004	0.948	3.409	0.065	2.824	0.090

397 df: degrees of freedom; Pseudo-F: F value by permutation (Anderson et al., 2005); P: significance of pseudo-
398 F with Monte Carlo correction. Significant differences are indicated in bold.

399



401
402 **Fig. 1 Location where corals were collected.** (a) Map of Calafuria (43°27' N, 10°21' E, Italy, Ligurian Sea).
403 (b) Specimens of the common and abundant coral *L. pruvoti* in a crevice at 16 m in Calafuria.

404 [to be printed in colour]

405

406

407

408

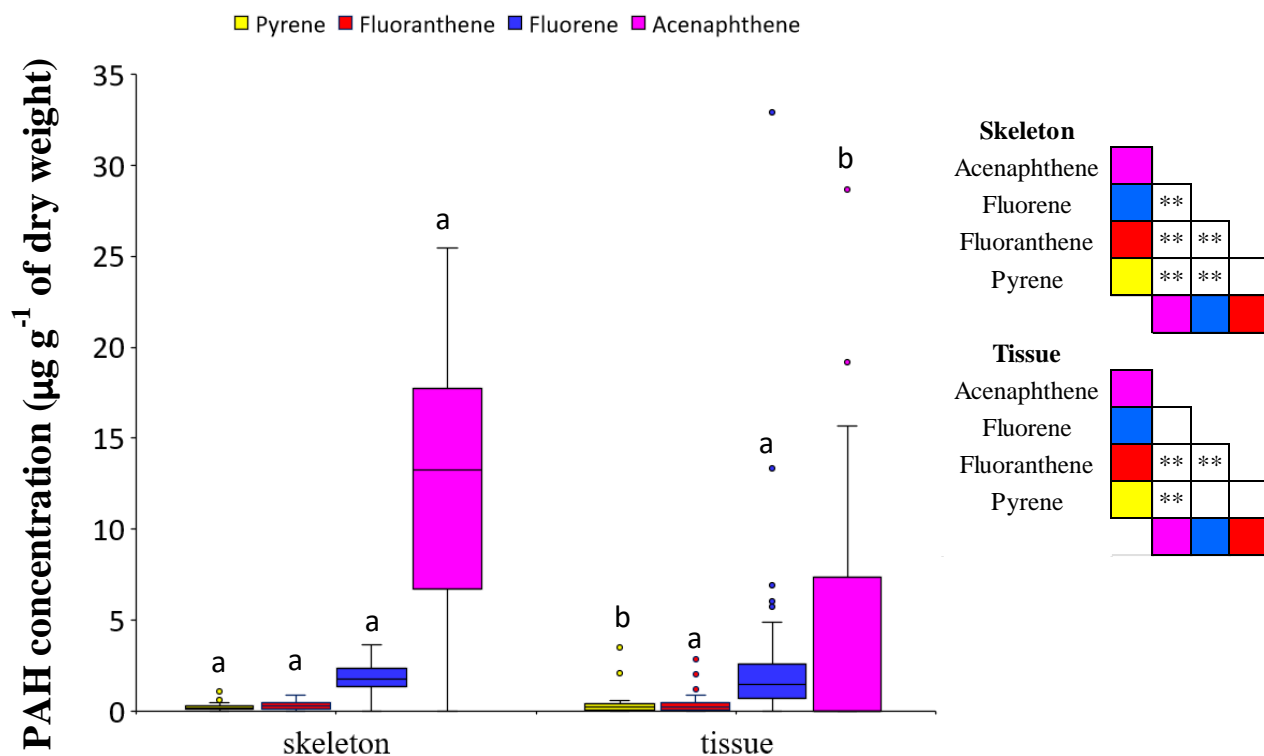


Fig. 2 Concentration ($\mu\text{g g}^{-1}$ of dry weight) of PAHs in the two biological compartments of *L. pruvoti*. (a) Boxplots represent median, upper and lower quartiles (N = 36) of PAH concentration in coral skeleton and tissue. Different letters indicate significant differences in the concentration of each PAH between biological compartments ($P < 0.05$; PERMANOVA pairwise comparisons t-tests; 999 permutations). (b) Within each biological compartment, triangular matrices report differences between pairs of PAHs (**P < 0.01; PERMANOVA pairwise comparisons t-tests; 999 permutations).

[to be printed in colour]

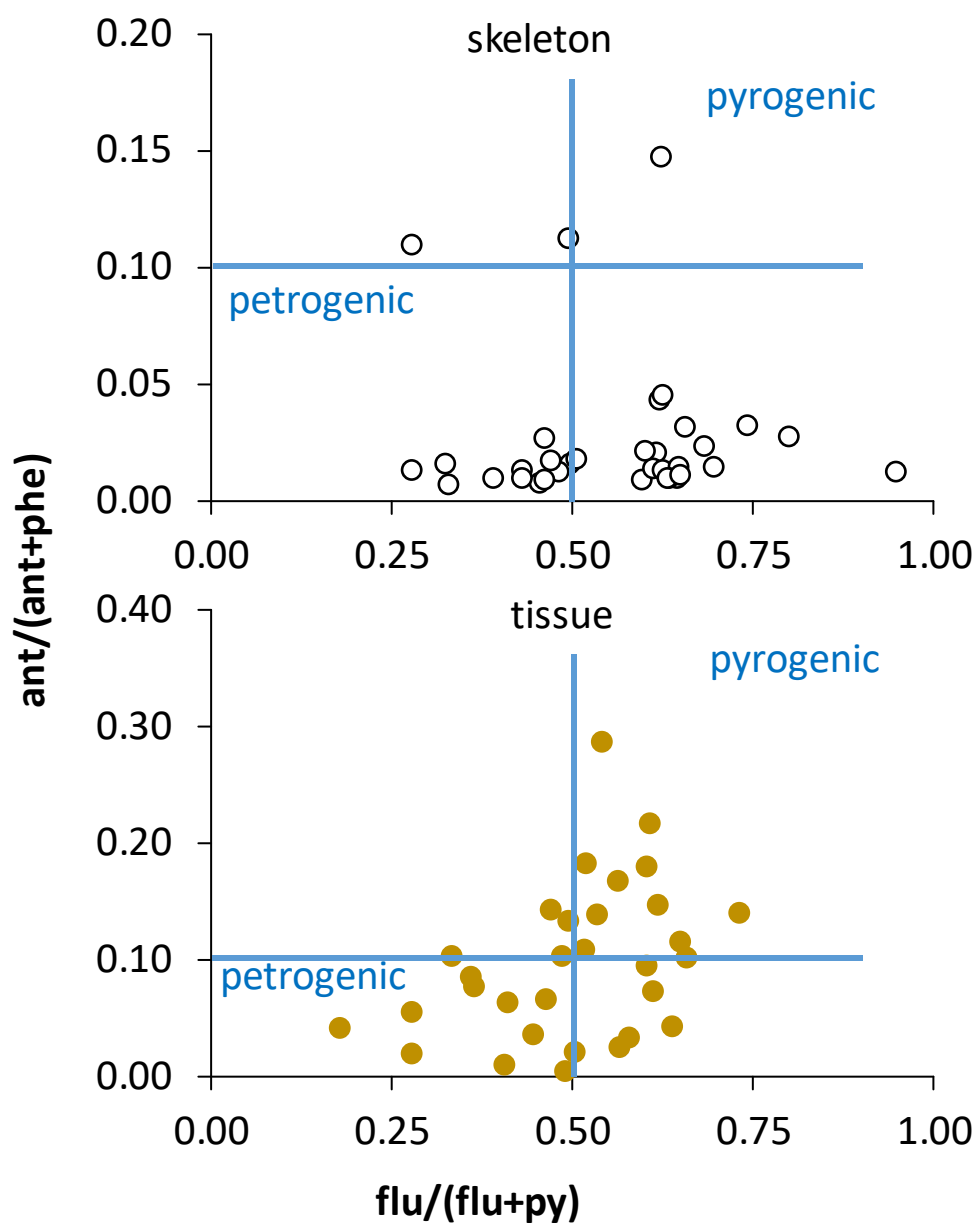
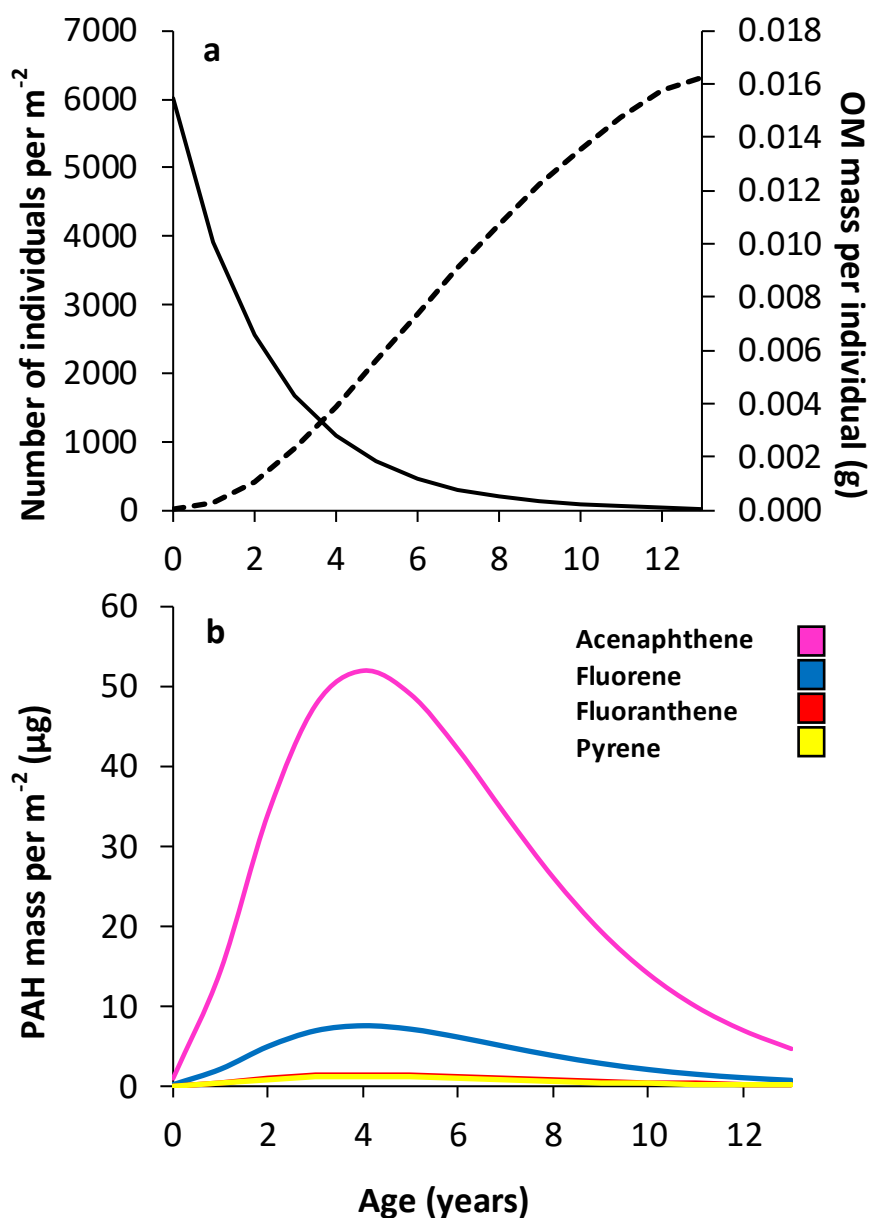


Fig. 3 Source implications of PAHs analyzed in the two biological compartments of *L. pruvoti*, using the PAH diagnostic ratios. Cross plots of the *anthracene/(anthracene+phenanthrene)* to *fluoranthene/(fluoranthene+pyrene)* ratios, the blue lines represent the petroleum/combustion transition point.

[to be printed in colour]



436

437 **Fig. 4 PAH storage in the skeletons of *L. pruvoti* in 1 m² of population at 16 m depth in Calafuria (Italy,**

438 **Ligurian Sea), according to population age structure. (a) Distribution of the number of individuals (solid**

439 **line), and OM mass (dotted line) with coral age. (b) PAH mass stored in the skeleton (blue = fluorene, pink =**

440 **acenaphthene, yellow = pyrene, red = fluoranthene) over the age of *L. pruvoti* specimens.**

441 *[to be printed in colour]*

442

443

444

445 **Table A.1** HPLC-FLD determination of selected PAHs: slope of the calibration curve, coefficient of
446 determination, limits of detection (LODs), limits of quantification (LOQs), and recovery (%).

PAH	slope	coefficient of determination (%)	LOD (ng mL ⁻¹)	LOQ (ng mL ⁻¹)	Recovery (%) (mean ± std. dev.)
acenaphthene	2.094	99.98	0.004	0.011	82 ± 10
fluorene	4.106	99.95	0.002	0.005	87 ± 7
fluoranthene	5.030	99.99	0.002	0.005	81 ± 7
pyrene	1.717	99.93	0.004	0.013	81 ± 5

463 **Table A.2** Length, Age and PAH concentration ($\mu\text{g g}^{-1}$ dry weight, d.w.) data in the two biological
 464 compartments of each sample of *L. pruvoti*. Samples are arranged in increasing age order.

Sample code	Length (mm)	Age (yr)	Biological compartment	acenaphthene ($\mu\text{g g}^{-1}$ d.w.)	fluorene ($\mu\text{g g}^{-1}$ d.w.)	fluoranthene ($\mu\text{g g}^{-1}$ d.w.)	pyrene ($\mu\text{g g}^{-1}$ d.w.)
LPRCL50	3.45	2.8	skeleton	20.2	3.62	0.215	0.257
			tissue	<LOQ	0.659	0.447	0.240
LPRCL10	4.00	3.4	skeleton	1.60	0.198	<LOQ	<LOQ
			tissue	<LOQ	0.774	0.277	0.241
LPRCL01	4.10	3.5	skeleton	16.8	2.29	0.329	0.199
			tissue	3.74	1.80	0.167	0.291
LPRCL38	4.35	3.8	skeleton	13.2	1.80	0.603	0.648
			tissue	15.7	13.4	0.920	1.34
LPRCL12	4.40	3.9	skeleton	9.03	1.48	0.151	0.154
			tissue	<LOQ	1.79	2.86	3.55
LPRCL13	4.40	3.9	skeleton	9.78	1.63	0.155	0.325
			tissue	<LOQ	1.55	0.380	0.250
LPRCL62	4.40	3.9	skeleton	13.5	1.15	0.289	0.177
			tissue	3.72	1.69	0.059	0.106
LPRCL69	4.50	4.0	skeleton	20.7	2.12	0.372	0.200
			tissue	11.4	1.80	0.067	0.096
LPRCL17	4.60	4.1	skeleton	8.44	1.94	0.337	0.210
			tissue	10.9	2.86	0.084	0.436
LPRCL32	4.60	4.1	skeleton	<LOQ	1.49	0.557	0.194
			tissue	<LOQ	4.87	0.824	0.600
LPRCL57	4.65	4.2	skeleton	15.7	2.43	0.711	1.11
			tissue	0.738	<LOQ	<LOQ	<LOQ
LPRCL39	4.70	4.3	skeleton	15.7	2.03	0.360	0.215
			tissue	<LOQ	0.827	0.836	0.968
LPRCL05	4.75	4.3	skeleton	<LOQ	<LOQ	<LOQ	<LOQ
			tissue	<LOQ	1.31	0.204	0.192
LPRCL34	4.80	4.4	skeleton	19.6	3.38	0.475	0.317
			tissue	7.23	2.11	<LOQ	0.246
LPRCL35	4.80	4.4	skeleton	3.94	2.05	<LOQ	<LOQ
			tissue	<LOQ	6.06	0.820	0.630
LPRCL45	4.80	4.4	skeleton	13.4	2.61	0.204	0.238
			tissue	7.40	2.66	0.280	1.30
LPRCL56	4.80	4.4	skeleton	25.4	1.36	0.371	0.203
			tissue	<LOQ	1.02	0.259	0.274
LPRCL02	4.85	4.5	skeleton	6.56	1.07	0.237	0.125
			tissue	<LOQ	1.58	0.163	0.103
LPRCL67	4.90	4.6	skeleton	24.5	2.35	0.431	0.251
			tissue	<LOQ	0.681	0.120	0.077
LPRCL75	4.95	4.6	skeleton	13.3	1.88	0.244	<LOQ
			tissue	<LOQ	1.28	0.238	0.243
LPRCL14	5.00	4.7	skeleton	25.4	2.61	0.418	0.282
			tissue	<LOQ	2.50	0.463	0.263
LPRCL11	5.05	4.8	skeleton	14.2	1.50	0.140	0.157
			tissue	<LOQ	0.708	0.120	0.093
LPRCL22	5.10	4.9	skeleton	15.9	1.81	0.612	0.267
			tissue	<LOQ	0.423	0.245	0.207
LPRCL42	5.10	4.9	skeleton	<LOQ	<LOQ	<LOQ	<LOQ
			tissue	19.2	6.95	<LOQ	<LOQ
LPRCL74	5.10	4.9	skeleton	6.14	0.820	0.100	0.117
			tissue	<LOQ	0.712	0.235	0.086
LPRCL59	5.25	5.1	skeleton	5.81	0.845	0.052	<LOQ
			tissue	<LOQ	0.572	0.262	0.161
LPRCL16	5.35	5.3	skeleton	<LOQ	2.59	0.914	0.938
			tissue	<LOQ	<LOQ	<LOQ	<LOQ
LPRCL07	5.40	5.3	skeleton	9.44	3.66	0.555	1.14
			tissue	15.1	2.94	0.573	0.297
LPRCL19	5.40	5.3	skeleton	18.1	2.27	0.517	0.285
			tissue	7.45	0.766	<LOQ	0.087
LPRCL58	5.50	5.5	skeleton	12.4	2.41	0.477	0.274
			tissue	<LOQ	0.51	0.077	0.050
LPRCL04	5.95	6.4	skeleton	7.13	0.386	0.289	0.173
			tissue	3.04	1.20	0.037	0.074
LPRCL30	5.95	6.4	skeleton	18.5	2.71	0.149	0.196
			tissue	8.69	2.41	<LOQ	<LOQ
LPRCL09	6.00	6.5	skeleton	20.3	1.75	0.353	0.468
			tissue	<LOQ	0.517	0.142	0.160
LPRCL64	6.20	6.9	skeleton	14.3	1.44	0.191	0.186
			tissue	28.6	32.9	2.04	2.12
LPRCL33	6.30	7.1	skeleton	10.7	1.56	0.309	0.196
			tissue	<LOQ	5.73	1.21	1.19
LPRCL08	6.50	7.6	skeleton	7.70	1.40	0.244	0.114
			tissue	<LOQ	1.45	0.345	0.320

465 LOQ: limit of quantification

467 **Table A.3** Results of the comparative PERMANOVA pairwise tests between PAHs within each biological
 468 compartment of *L. pruvoti* (999 permutations).

PAHs	Skeleton		Tissue	
	T	P	t	P
acenaphthene vs fluorene	6.555	0.001	0.352	0.729
acenaphthene vs fluoranthene	7.549	0.001	2.189	0.028
acenaphthene vs pyrene	7.565	0.001	2.134	0.046
fluorene vs fluoranthene	7.483	0.001	2.053	0.040
fluorene vs pyrene	7.494	0.001	1.987	0.051
fluoranthene vs pyrene	0.394	0.664	0.399	0.651

469 t: t-Statistics; P: significance of t with Monte Carlo correction. Statistically significant values are in bold (P <
 470 0.05).

471

472 **Table A.4** Results of the comparative PERMANOVA pairwise tests between biological compartments within
 473 each PAH of *L. pruvoti* (999 permutations).

Biological compartments	acenaphthene		fluorene		fluoranthene		pyrene	
	t	P	t	P	t	P	t	P
Skeleton vs Tissue	3.930	0.001	1.034	0.312	1.852	0.067	2.217	0.021

474 t: t-Statistics; P: significance of t with Monte Carlo correction. Significant differences are indicated in bold.

475

476

477

478

479

480

481

482

483

484

485

486

487

488

489

490 **Table A.5** Mass of PAHs stored in the skeletons of *L. pruvoti* in 1 m² of the Calafuria population at 16 m
 491 depth. Data for *B. europaea* in the same site at 6 m are added for comparison (Caroselli et al., 2020). The
 492 number of age classes for the two species matches their estimated maximum individual lifespan.

Coral age (yr), t	Coral mean length (mm), L_t	Coral sk. mass (g), M_t	Coral sk. OM (mg), $M_{OM(t)}$	N of corals per m ² , N_t	Cumulative OM (g m ⁻²)	acenaphthene (µg m ⁻²)	fluorene (µg m ⁻²)	fluoranthene (µg m ⁻²)	pyrene (µg m ⁻²)
<i>Leptopsammia pruvoti</i>									
0	0.7	0.001	0.013	6004	0.1	1.0	0.2	0.03	0.02
1	2.1	0.012	0.30	3918	1.2	15	2.1	0.38	0.32
2	3.2	0.043	1.1	2557	2.8	34	5.0	0.89	0.75
3	4.1	0.093	2.3	1669	3.9	48	7.0	1.2	1.1
4	4.8	0.155	3.9	1089	4.2	52	7.6	1.4	1.1
5	5.5	0.224	5.6	711	4.0	49	7.2	1.3	1.1
6	6.0	0.295	7.4	464	3.4	42	6.2	1.1	0.92
7	6.4	0.364	9.1	303	2.7	34	5.0	0.88	0.74
8	6.8	0.429	11	198	2.1	26	3.8	0.68	0.57
9	7.1	0.488	12	129	1.6	19	2.3	0.50	0.43
10	7.4	0.542	14	84	1.1	14	2.1	0.37	0.31
11	7.6	0.589	15	55	0.8	10	1.5	0.26	0.22
12	7.7	0.630	16	36	0.6	7.0	1.0	0.18	0.15
13	7.8	0.649	16	23	0.4	4.7	0.7	0.12	0.10
Total PAH mass						360	52	9.2	7.8
<i>Balanophyllia europaea</i>									
0	1.1	0.002	0.07	7.0	0.0005	0.00008	0.0001	0.000004	0.00002
1	3.2	0.036	1.0	5.3	0.0055	0.00093	0.0012	0.000046	0.00020
2	5.1	0.114	3.3	4.0	0.013	0.0023	0.0029	0.00011	0.00050
3	6.8	0.236	6.8	3.1	0.021	0.0036	0.0046	0.00018	0.00078
4	8.4	0.393	11	2.3	0.027	0.0045	0.0058	0.00022	0.00098
5	9.7	0.576	17	1.8	0.030	0.0050	0.0065	0.00025	0.0011
6	10.9	0.777	23	1.3	0.030	0.0052	0.0067	0.00026	0.0011
7	12.0	0.989	29	1.0	0.030	0.0050	0.0064	0.00025	0.0011
8	13.0	1.205	35	0.78	0.027	0.0046	0.0060	0.00023	0.0010
9	13.9	1.421	41	0.59	0.024	0.0041	0.0053	0.00020	0.0009
10	14.6	1.633	47	0.45	0.021	0.0036	0.0047	0.00018	0.0008
11	15.3	1.838	53	0.34	0.018	0.0031	0.0040	0.00015	0.0007
12	16.0	2.034	59	0.26	0.015	0.0026	0.0034	0.00013	0.0006
13	16.5	2.219	64	0.20	0.013	0.0021	0.0028	0.00011	0.0005
14	17.0	2.394	69	0.15	0.010	0.0018	0.0023	0.00009	0.0004
15	17.5	2.557	74	0.11	0.008	0.0014	0.0018	0.00007	0.0003
16	17.9	2.708	79	0.09	0.007	0.0011	0.0015	0.00006	0.0003
17	18.2	2.848	83	0.07	0.005	0.0009	0.0012	0.00005	0.0002
18	18.6	2.977	86	0.05	0.004	0.0007	0.0009	0.00004	0.0002
19	18.9	3.096	90	0.04	0.003	0.0006	0.0007	0.00003	0.0001
20	19.1	3.201	93	0.03	0.003	0.0005	0.0006	0.00002	0.0001
Total PAH mass						0.054	0.070	0.0027	0.0012